New Synchronization Method for Three-Phase PWM Rectifiers

ROBINSON FIGUEIREDO DE CAMARGO HUMBERTO PINHEIRO

Grupo de Eletrônica de Potência e Controle, Federal University of Santa Maria
CEP 97105-900, Santa Maria, RS, BRAZIL, +55-55-220-8463

Abstract – This paper proposes a new *open-loop* synchronization method for three-phase pwm rectifiers connected to the utility grid. It presents a better performance if compared with other *open-loop* methods in the presence of grid voltage unbalance and harmonics. Moreover, it reduces the total harmonic distortion (*THD*) and it does not require complex algorithms such as phase-locked loop (*PLL*). Simulation results and abacuses are given to demonstrate the good performance of the proposed method if compared to the well known modified synchronous reference frame method. Simulation results from a three-phase PWM rectifier with deadbeat controller are given to demonstrate the performance of the proposed method.

KEYWORDS – normalized voltage, positive sequence, synchronous frame, three-phase PWM rectifiers.

1 Introduction

Several techniques to synchronize three-phase PWM rectifier to the utility grid have been reported. They can be classified as *closed-loop* [1-5] and the *open-loop* [6-13] methods. In *closed-loop* methods the angle of synchronism is obtained through a closed-loop structure, which aimed at locking the estimated value of the phase angle to its actual value. On the other hand, *open-loop* synchronization methods, the synchronism angle or normalized synchronism vector is obtained directly from the grid voltages [6, 7, 9], virtual flux [8, 10, 11] or estimate grid voltages [12, 13].

Although *closed-loop* methods have low sensitivity to the grid frequency, a trade off between good transient response and good filtering characteristics must always be considered. Moreover, the implementation and design *closed-loop* methods are usually more complex than the *open-loop* counterparts.

Among the *open-loop* methods the modified synchronous reference frames (*MSRF*) [6, 7] and the low-pass filter based (*LPF-B*) methods [9] standout for their simplicity. The main attribute of the former is to be independent of the grid frequency, however it presents a poor performance in terms of current *THD* under unbalance and harmonics in the grid voltage. The later is less sensitive to the grid harmonics. However, all *open-loop* methods reported so far have a poor performance under grid voltage unbalance [5], increasing the harmonic distortion [14] of the input current.

This paper proposes a new *open-loop* synchronization method for three-phase PWM rectifier connected to the utility grid that provides a good performance in terms of input current *THD* of three-phase PWM rectifiers even in the presence of harmonics and severe unbalance in the grid voltages. It is simpler than *closed-loop* methods and can be applied for three-phase PWM converters connected to the utility grid. Simulation, abacus and results are given to demonstrate the *THD* and unbalance factor of the PWM rectifier input currents using the new method and compared with a classic *MSRF* method.

2 Proposed Synchronization Method

The proposed method is called normalized positive sequence reference frames, *NPSF*, and it is shown in Fig. 1 for three-phase three-wire systems, where just two line-to-line voltages are measured.

In the *NPSF* method the vector formed by line-to-line grid voltages, $\mathbf{v}_{l\text{-}l}$ (1), is first filtered, using the low pass filter (LPF_1), which generate a filtered voltage vector, $\mathbf{v}_{l\text{-}l\_fic}$, with same amplitude but phase-shift by 90º degree at the fundamental frequency.

$$\mathbf{v}_{l-l} = \begin{bmatrix} v_{ab} \\ v_{bc} \end{bmatrix}, \tag{1}$$

Then, the $\mathbf{v}_{l\text{-}l\_fic}$ is again filtrated by using a second low pass filter, LPF_2, which provides an additional 90º phase-shift. These results in a new filtered line-to-line voltage vector, $\mathbf{v}_{l\text{-}l\_new}$, with same amplitude but phase-shift by 180º with respect the original vector $\mathbf{v}_{l\text{-}l}$.

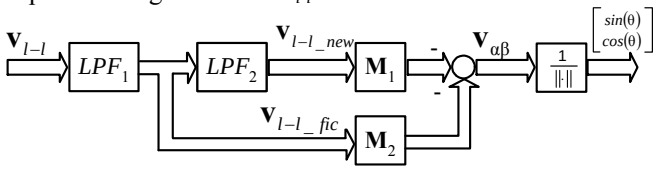

Fig. 1 – Proposed normalized positive sequence reference frame for three-phase three-wire systems.

The vector formed by αβ stationary voltages of positive sequence filtrated, $\mathbf{v}_{\alpha\beta}=[v_\alpha \; v_\beta]^T$, is obtained by multiplication of voltage vector $\mathbf{v}_{l\text{-}l\_new}$ and $\mathbf{v}_{l\text{-}l\_fic}$ by the matrices $\mathbf{M}_1$, (3), and $\mathbf{M}_2$, (4) respectively, as follow:

$$\mathbf{v}_{\alpha\beta} = -\left(\mathbf{M}_1\mathbf{v}_{l\text{-}l\_new} + \mathbf{M}_2\mathbf{v}_{l\text{-}l\_fic}\right), \tag{2}$$

where:

$$\mathbf{M_1} = \frac{1}{2}\begin{bmatrix} \sqrt{6}/3 & \sqrt{6}/6 \\ 0 & \sqrt{2}/2 \end{bmatrix}, \tag{3}$$

$$\mathbf{M}_2 = \frac{1}{2}\begin{bmatrix} 0 & \sqrt{2}/2 \\ -\sqrt{6}/3 & -\sqrt{6}/6 \end{bmatrix}. \quad (4)$$

The matrices $\mathbf{M}_1$ and $\mathbf{M}_2$ are obtaining by the combination of three transformations that are: (i) the αβ transformation, (ii) positive sequence transformation [5] and (iii) line-to-phase transformation.

Then, the entries of the normalized the $\mathbf{v}_{\alpha\beta}$ is obtained as follow:

$$v_{x\_n} = \frac{v_x}{\left\|\mathbf{v}_{\alpha\beta}\right\|}, \quad (5)$$

where, x denote α or β quantities and the norm is given by:

$$\left\|\mathbf{v}_{\alpha\beta}\right\| = \sqrt{v_\alpha^2 + v_\beta{}^2}\ . \quad (6)$$

It is possible to obtain the normalized synchronism vector, $\mathbf{v}_{\alpha\beta\text{-}n}=[v_{\alpha\text{-}n}\ \ v_{\beta\text{-}n}]^T$, whose components are the *sine* and *cosine* quantities as follow:

$$sin(\theta) = v_{\beta\_n} \text{ and } cos(\theta) = v_{\alpha\_n}, \quad (7)$$

where $\theta=2\pi f$ an estimated of the grid voltage of fundamental frequency.

These quantities are used to synchronize the input currents in the PWM rectifiers with the grid voltages.

Next, the design of LPF_1 and LFP_2 used in new method is presented.

2.1 Low Pass Filter Design

The LPF_1 and LPF_2 are design the same manner, however with distinct purposes. A second order *LPF* is design for both cases to provide unit gain and phase-shift of 90-degree of the fundamental frequency as shown in Fig. 2. It operates in 60 Hz (377 rad/sec) and the transfer function in time domain is given by:

$$G(s) = \frac{\omega_n^2}{s^2 + 2\zeta\omega_n s + \omega_n^2}, \quad (8)$$

where: $\omega_n=2\pi f$ and f=60 Hz.

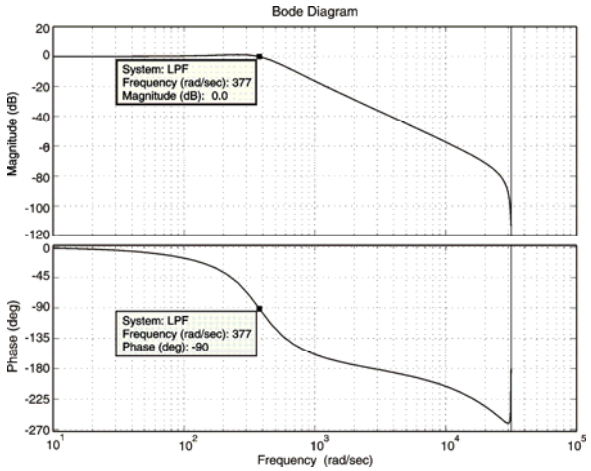

Fig. 2 – Bode diagram of the LPF_1 *or* LPF_2 designed to operated with frequency (rad/sec)= 377, magnitude(dB) = 0 dB and phase(deg) = -90º, where the filter parameters are $\omega_n=2\pi f$, f=60 Hz and ζ=0.5.

The frequency sensitivity of the proposed method depends on the selected damping ratio, ξ. Here a damping ratio of 0.5 has been chosen. This sensitivity is not concern since usually public utility grid frequency in stead-state is kept within ± 1 Hz of this nominal value as mentioned in IEC 61000-2-2.

3 Comparative Analysis

This section compares the *NPSF* method with a typical *open-loop* method. The *MSRF* have been selected since they present similar principle and performance. The current control technique by decoupling by state feedback plus servo controller (*DCT*) is used in synchronous frame (*SF*) applied in three-phase PWM rectifiers. In this case the input currents of these converters are synchronized with the grid voltages. Then the *NPSF* and *MSRF* methods are applied to verify the difference between both methods. Fig. 4 showed the block diagram of algorithms and controller for three-phase PWM rectifiers that used the *NPSF* or *MSRF* methods

Two performance criteria are select to compare both methods, *THD* and unbalance factor in the input currents of the PWM rectifiers under unbalance and harmonics in the grid voltages. These criteria are present in the APPENDIX.

Below the basic equations and the block diagram of the controller used are presented as well as the simulation results.

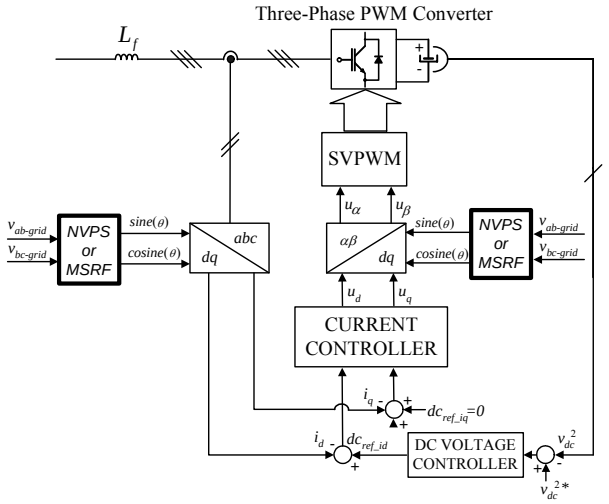

Fig. 3 – Block diagram of algorithms and controllers for three-phase three-wire PWM rectifiers used the *NPSF* or *MSRF* methods.

3.1 Decoupling by State Feedback Plus Servo Controller (DCT)

The theory of the decoupled by state feedback very well discuss in [15-18]. This is based in the obtaining of decoupling matrixes $\mathbf{M}_{des}$ and $\mathbf{K}_{des}$, so that three-phase PWM rectifier can be represented as two SISO, as shown in the Fig.4. This controller include the design the servo controllers for *d* and *q* axis guarantee the zero error in steady state due to presence of the grid voltages, consider as disturbance.

More detail about the design of matrixes $\mathbf{M}_{des}$, $\mathbf{K}_{des}$ and $\mathbf{R}_p$, as well as the design of the servo gains in the axis *d* and *q* are presented in [17, 18]

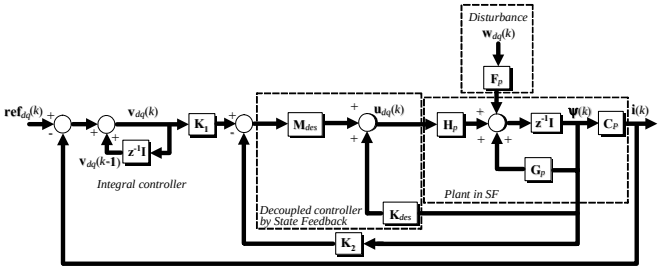

Fig. 4 – Basic scheme for decoupled controller by state feedback plus servo controllers in SF.

The main equations in discrete domain are:
The state vectors:

$$\mathbf{u}_{dq\_des}(k) = \mathbf{M}_{des}\left[u_d(k-1)\;\; u_q(k-1)\right]^{\mathrm{T}} + \mathbf{K}_{des}\boldsymbol{\psi}(k), \quad (9)$$

where: $\boldsymbol{\psi}(k) = \left[\mathbf{i}_{dq}(k-1)\;\; \mathbf{u}_{dq\_des}(k-1)\right]^{\mathrm{T}}$.

The state vectors:

$$u_x(k) = k_{1x}v_x(k) - k_{2x}\left[i_x(k)\;\; u_x(k-1)\right]^{\mathrm{T}}, \quad (10)$$

Reference of the d axis at the internal current loop:

$$dc_{ref\_id}(k) = u_{cc}(k), \quad (11)$$

State equation of the integrator is:

$$v_x(k) = v_x(k-1) + dc_{ref\_ix}(k) - i_x(k), \quad (12)$$

state equation of the integrator. Note that the subscript *x* represents *d* or *q* axis.

Figs. 5-24 shown the simulation results used the *NPSF* and *MSRF* in the *DCT* controller. It is possible to observer that under grid voltage balance, Fig. 5 and Fig. 6, both techniques present similar performance in terms of *THD* and unbalance in the input currents of the rectifiers.

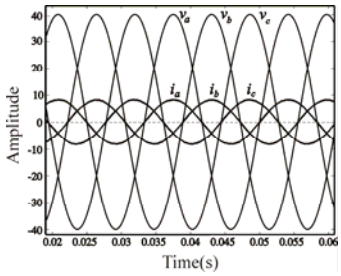

Fig. 5 – Phase-to-neutral grid voltages under 0 % of unbalance and phase-to-neutral input currents of the rectifiers used the *DCT* current controller and the *NPSF* method. THD_i=1.606 %, *Unb*%=0 %.

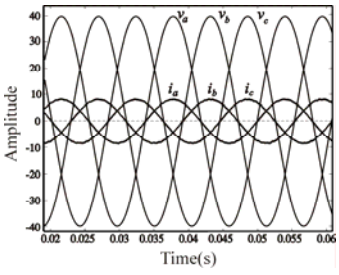

Fig. 6 – Phase-to-neutral grid voltages under 0 % of unbalance and phase-to-neutral input currents of the rectifiers used the *DCT* current controller and the *MSRF* method. THD_i=1.606 %, *Unb*=0 %.

However, under grid voltages unbalance, as shown in Fig. 7 and Fig. 8, the new *NPSF* method reduce the unbalance and harmonic components significantly, as shown in harmonic spectral of the Fig. 9, if compared with the *MSRF* method whose harmonic spectral is showing in the Fig. 10. In this case a severe unbalance, 25%, in the grid voltages was considered here to emphasize the differences between these methods. Figs. 11 and 12 present the *sine* and *cosine* generate used the *NPSF* and *MSRF* respectively, where it is possible to see that the *sine* and *cosine* generate used the *NPSF* is not present significant distortions same under severe grid voltage unbalance.

Figs. 13 and 14 present the grid voltages with harmonic distortion, in the utility voltages the *THD* is typically less than 5%. In this case is consider a *THD*=5% in the grid voltages and the presence of 5ª, 7ª and 11ª harmonics with the same amplitude. Fig. 15 presents the harmonic spectral of the input current of the rectifier, where the *THD* of the current when *NPSF* method is used it is reduce significantly if compared with Fig. 16 that used the *MSRF* method. Moreover, the *sine* and *cosine* generate used the *NPSF*, Fig. 17, it is not present significant distortions same under grid voltage harmonics if compared the Fig. 18 that used the *MSRF* method.

Figs. 19 and 20 present a case where 25% of unbalance and 5% of *THD* are consider in the grid voltages used the *NPSF* and *MSRF* methods respectively. It is possible to see in the harmonic spectral of the input currents in the Fig. 21 used the *NPSF* method that the *THD* of currents are reduced if compared the Fig. 22 that used the *MSRF* method. Furthermore the *sine* and *cosine* generated used the *NPSF* method, Fig. 23, it is not present significantly distortions if compared the Fig. 24 that *sine* and *cosine* is generated to use the *MSRF* method.

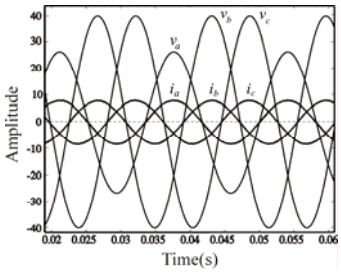

Fig. 7 – Phase-to-neutral grid voltages under 25% of unbalance and phase-to-neutral input currents of the rectifiers used the *DCT* current controller and the *NPSF* method *Unb*%=1.554 %.

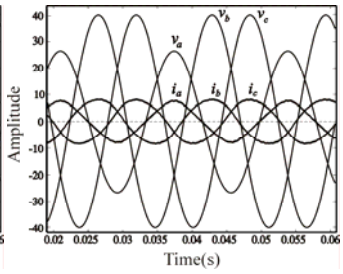

Fig. 8 – Phase-to-neutral grid voltages under 25% of unbalance and phase-to-neutral input currents of the rectifiers used the *DCT* current controller and the *MSRF* method *Unb*%=6.185 %.

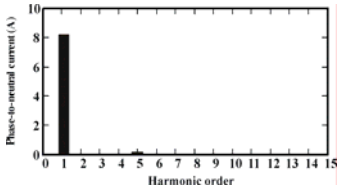

Fig. 9 – Harmonic spectral of *a* phase-to-neutral current of the Fig. 6, where the *THDi*=1.494 %.

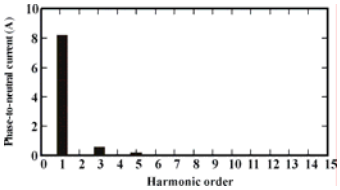

Fig. 10 – Harmonic spectral of *a* phase-to-neutral current of the Fig. 7, where the *THDi*=6.749 %.

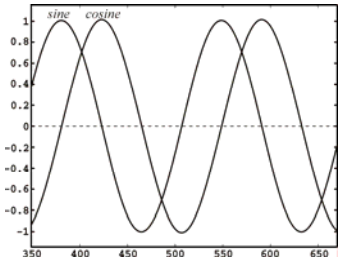

Fig. 11 – *Sine* and *cosine* generate by *NPSF* method with 25 % of grid voltage unbalance.

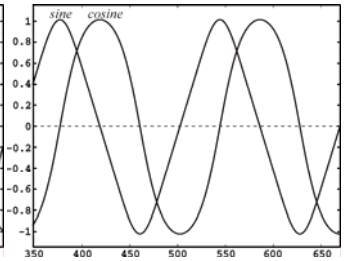

Fig. 12 – *Sine* and *cosine* generate by *MSRF* method with 25 % of grid voltage unbalance.

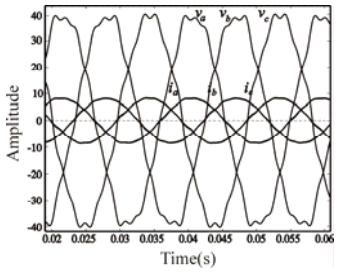

Fig. 13 – Phase-to-neutral grid voltages under THD*v*=5.0 %, and phase-to-neutral input currents of the rectifiers used the *DCT* current controller and the *NPSF* method.

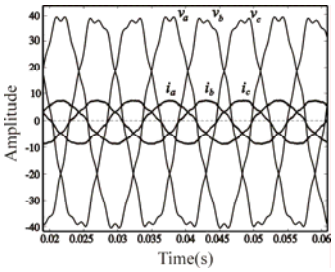

Fig. 14 – Phase-to-neutral grid voltages under THD*v*=5.0 %, and phase-to-neutral input currents of the rectifiers used the *DCT* current controller and the *MSRF* method.

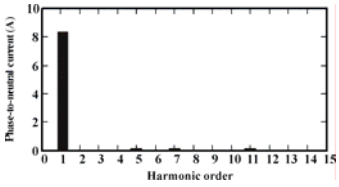

Fig. 15 – Harmonic spectral of *a* phase-to-neutral current of the Fig. 12, where the THD*i*=2.49 %.

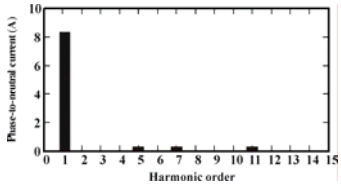

Fig. 16 – Harmonic spectral of *a* phase-to-neutral current of the Fig. 13, where the THD*i*=5.0 %.

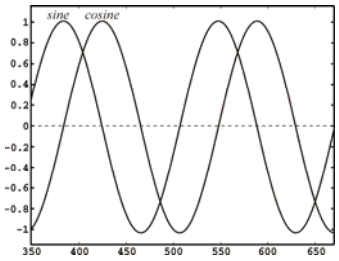

Fig. 17 – Sine and cosine generate by *NPSF* method with THD*v*=5.0 % of the grid voltages.

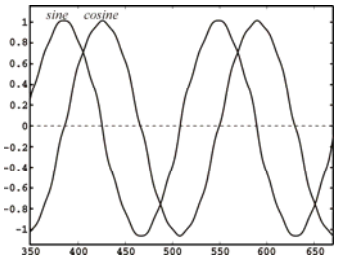

Fig. 18 – Sine and cosine generate by *MSRF* method with THD*v*=5.0 % of the grid voltages.

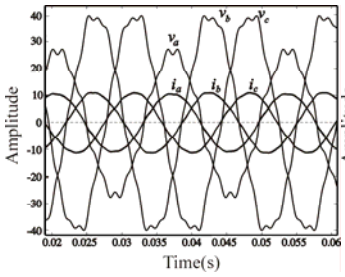

Fig. 19 – Phase-to-neutral grid voltages under 25 % of unbalance and THD*v*=5.0 % and phase-to-neutral input currents of the rectifiers used the *DCT* current controller and the *NPSF* method, Unb%=1.554 %.

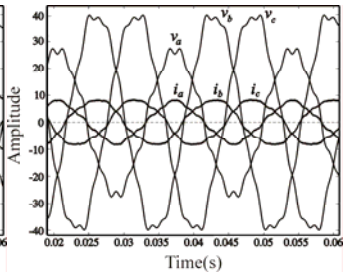

Fig. 20 – Phase-to-neutral grid voltages under 25 % of unbalance and THD*v*=5.0 % and phase-to-neutral input currents of the rectifiers used the *DCT* current controller and the *NPSF* method. Unb%=6.185 %.

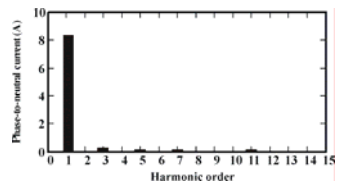

Fig. 21 – Harmonic spectral of *a* phase-to-neutral current of the Fig. 18, where the *THDi*=4.63 %.

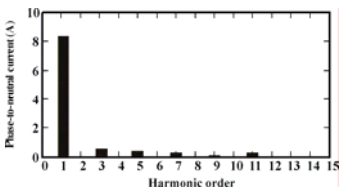

Fig. 22 – Harmonic spectral of *a* phase-to-neutral current of the Fig. 19, where the *THDi*=8.38 %.

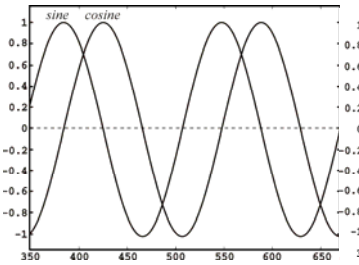

Fig. 23 – Sine and cosine generate by *NPSF* method with 25 % of unbalance and THD*v*=5.0 % of the grid voltages.

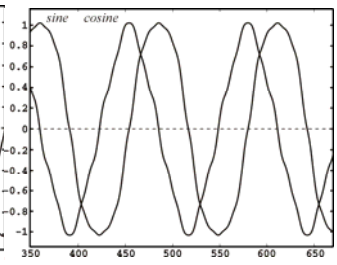

Fig. 24 – Sine and cosine generate by *MSRF* method with 25 % of unbalance and THD*v*=5.0 % of the grid voltages.

The next section presents a comparative analysis in terms of unbalance and *THD* performances in the input currents of the rectifiers under unbalance variation in the grid voltages used the *NPSF* and *MSRF* in the *DCT* controllers applied in three-phase PWM rectifiers.

4. UNBALANCE VARIATION OF THE GRID VOLTAGES

As commented in the previous section the main problem of the *open-loop* methods is the poor performance under grid voltage unbalance. In this section, this problem is more emphasized, through a comparison analysis between the *NPSF* and *MSRF* methods, which are used in the *DCT* current controller under unbalance variation of the grid voltages. The performance of the input currents of the rectifiers is investigated in terms of unbalance factor and *THD*.

Fig. 25 presents the abacus of the unbalance variations of the grid voltages versus unbalance variations of the input currents of the rectifier used *NPSF* and *MSRF* methods in the *DCT* current controller. It is possible to observer that for unbalance voltages larger than 2% the *NPSF* techniques is better than *MSRF* technique, where the first presents a smaller percentage of unbalance.

Fig. 26 presents the unbalance variations of the grid voltages versus *THD* of the input currents of the rectifier used *NPSF* and *MSRF* methods applied in the *DCT* controller. It is possible to verify that for all unbalance variation of the grid voltages used here, the *NPSF* method is better than *MSRF* technique, where the first presents a smaller percentage of THD_i.

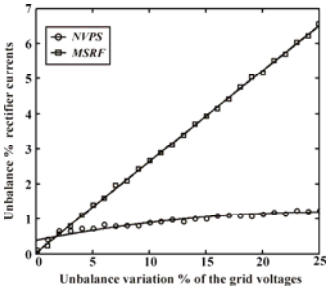

Fig. 25 – Abacus of the *Unb*% of the grid voltages versus *Unb*% of the input currents to the rectifiers used *NPSF* and *MSRF* method applied in the *DCT* controller.

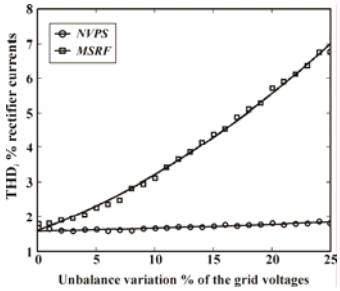

Fig. 26 – Abacus of the *Unb* % of the grid voltages versus *THD*% of the input currents to the rectifiers used *NPSF* and *MSRF* methods applied in the *DCT* controller.

5 Experimental Results

This section presents experimental results used the *MSRF* methods in the *DCT* current control technique applied in the three-phase PWM rectifier. The experimental setup operate as sampling and switching frequency with 10 kHz, design inductor with L=2.50 mH and fundamental frequency of the main operated in 60 Hz. The DSP TMS320F241 was used to the implementation of the control algorithms, mainly due it good performance and low cost.

The Fig. 27 *a* and *b* exhibit the experimental results of the phase-to-neutral grid voltages and input currents of the rectifier used the *MSRF* controller under THD_v=2.5% and 5.8 % of unbalance in the grid voltages and the Fig. 28 presents the harmonic spectral of the *a* phase-to-neutral current of the Fig. 28, which presents THD_i=1.9 %.

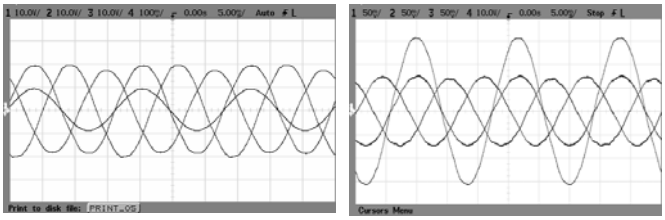

(a) (b)

Fig. 27. Experimental results of the *DCT* controller, rectifier operated with unit power factor. (a) Phase-to-neutral grid voltages and *a* phase-to-neutral current of rectifier. Horizontal scale: 5 ms/div. Vertical scale of currents: 10 A/div. Vertical scale of voltage:10 V/div. (b) Phase-to-neutral current of rectifier and *a* phase-to-neutral grid voltage. Horizontal scale: 5

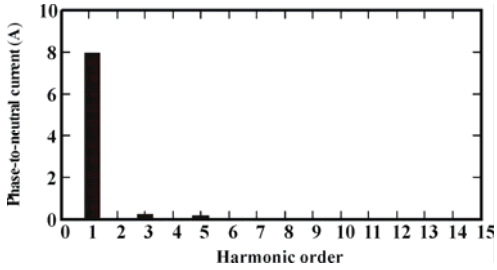

Fig. 28 – Harmonic spectral of *a* phase-to-neutral current of the Fig. 27 b, Unb%= 1.1 % andTHD*i*=1.9.

6. Conclusions

In this paper a new method of synchronization for PWM converters connected to the utility under unbalance and harmonics grid voltages is proposed. This *NPSF* method presents a better performance in terms of generation of *sine* and *cosine* if compared the others *open-loop* methods under unbalance in the grid voltages. Moreover, this method presents good results in the presence of harmonic distortion in the grid voltages. The *NPSF* and *MSRF* methods are compared used these method in *DCT* current controllers applied in three-phase PWM rectifiers. The performance of this controller used both methods are investigated in terms of *THD* and unbalance of the input currents of the rectifiers under unbalance and harmonics distortion of the grid voltages. Simulation results and abacus generated confirm that the *NPSF* reduce the THD_i and unbalance in the input current of the rectifier significantly. Experimental results of the *MSRF* method under unbalance and harmonic of the grid voltages are present to verify this problem.

Appendix

Comparative criteria select to compare *NPSF* and *MSRF* methods applied in three-phase PWM rectifiers:

Harmonics in the input currents of the rectifier: for this the *THD* of currents are used. It is defined in the *IEEE Std.* 519-1992, as follow:

$$THD_i\ \% = \left(\sqrt{\sum_{h=2}^{\infty} I_h^2} \Big/ I_1 \right) 100\ ; \qquad (13)$$

Current unbalance in the input currents of the rectifier: current unbalance can be defined as the maximum deviation from the average of the three-phase current, divided by average of the three-phase current, as definition in the *IEEE Std.*1159-1995, that is:

$$Unb\ \% = \left[\left(\left| I_{frms} - I_{avg} \right|_{\max} \right) \Big/ I_{avg} \right] 100 \cdot \qquad (14)$$

References:

[1] G.-C. Hsieh and J. C. Hung, "Phase-locked loop techniques – A survey," *IEEE Trans. on Industrial Electronics*, vol. 43, Dec. 1996, pp. 609-615.

[2] S.-J. Lee, J.-K. Kang and S.-K. Sul, "A new phase detecting method for power conversion systems considering distorted conditions in power system," *in Proc. IAS '99*, 1999, pp. 2167 – 2172.

[3] Costa, D. R. Jr., Rolim L.G.B. and Aredes M., "Analysis and software implementation of a robust synchronizing circuit PLL circuit," *in Proc. ISIE '03*, 2003, pp. 292 – 297.

[4] S. M. Deckmann, F. P. Marafão and M. S. de Pádua, "Single and three-phase digital PLL structures based on instantaneous power theory," *in Proc. COBEP'03*, 2003, Brazil, pp. 225-230.

[5] M. Karimi-Ghartemani and M. R. Iravani, "A method for synchronization of power electronic converters in polluted and variable-frequency environments," *IEEE Trans. on Power Systems*, vol. 19, Aug. 2004, pp. 1263-1270.

[6] V. Soares and G. D. Marques, "Active power filter control circuit based on the instantaneous active and reactive current id-iq method," *in Proc. PESC'97*, 1997, pp. 1096-1101.

[7] G. D. Marques, "A comparison of active power filter control methods in unbalanced and non-sinusoidal conditions," *in Proc. IECON'98*, 1998, pp. 444-449.

[8] J. L. Duarte, A. V. Zwam, C. Wijnands and A. Vandenput, "Reference frames fit for controlling PWM rectifiers," *IEEE Trans. on Industrial Electronics*, vol. 46, Jun. 1999, pp. 628-630.

[9] J. Svensson, “Synchronization methods for grid-connected voltage source converters,” *IEE Proceedings Generation Transmission and Distribution*, vol. 148, May 2001, pp. 229-235.

[10] M. Malinowski and M. P. Kazmierkowski, “DSP implementation of direct power control with constant switching frequency for three-phase PWM rectifiers,” *in Proc. IECON'02*, 2002, pp. 198-449.

[11] S. Hansen, M Malinowski, F Blaabjerg and M. P. Kazmierkowski, “Sensorless control strategies for PWM rectifier,” *in Proc. APEC'00*, 2000, pp. 832-838.

[12] R. M. Kennel, M. Linke and P. Szczupak, “Sensorless control of 4-quadrant-rectifiers for voltage source inverters (VSI),” *in Proc. PESC'03*, 2003, pp. 1057-1062.

[13] P. Szczupak and R. Kennel, “Sensorless control of PWM rectifiers by distorced suplly voltage,” *in Proc. PESC'04*, 2004, pp. 203-206.

[14] D. P. Manjure and E. B. Makram, “Impact of unbalance on power system harmonics,” *in Proc. ICHQP'02*, 2002, pp. 328-333.

[15] M. P. Kazmierkowski and L. Malesani, “Current control techniques for three-phase voltage-source PWM converters: a survey,” *IEEE Trans. on Industrial Electronics*, vol. 45, Oct. 1998, pp. 691-703.

[16] Falb P. L. and Wolovich W. A., “Decoupling in the design and synthesis of multivariable control systems”, *IEEE Transactions on Automatic Control*, vol. AC-12, Dec. 1967, pp. 651-659.

[17] R. F. Camargo, F. Botterón, M. H. Duarte, J. Marques, H. Pinheiro, “Análise e implementação de retificadores PWM trifásicos com resposta deadbeat utilizando desacoplamento por retroação de estados,” *in proc. CBA ’04*, 2004, in CD-ROM.

[18] R. F. Camargo and H. Pinheiro, “Deadbeat decoupled controller by state feedback for three-phase PWM rectifiers and comparative stability analysis,” *in. Proc. INDUSCON’04*, 2004, in CD-ROM.